Available online at www.sciencedirect.com

SCIENCE DIRECT

Biochimica et Biophysica Acta 1665 (2004) 142–155

BIOCHIMICA ET BIOPHYSICA ACTA
BBA

http://www.elsevier.com/locate/bba

Vesicle size-dependent translocation of penetratin analogs across lipid membranes

Daniel Persson[a,*], Per E.G. Thorén[a], Elin K. Esbjörner[a], Mattias Goksör[b], Per Lincoln[a], Bengt Nordén[a]

[a]*Department of Chemistry and Bioscience, Chalmers University of Technology, SE-412 96 Gothenburg, Sweden*
[b]*Department of Experimental Physics, Chalmers University of Technology, SE-412 96 Gothenburg, Sweden*

Received 20 November 2003; received in revised form 16 July 2004; accepted 22 July 2004
Available online 25 August 2004

Abstract

The recent discoveries of serious artifacts associated with the use of cell fixation in studies of the cellular uptake of cell-penetrating peptides (CPPs) have prompted a reevaluation of the current understanding of peptide-mediated cellular delivery. Following a report on the differential cellular uptake of a number of penetratin analogs in unfixed cells, we here investigate their membrane translocation abilities in large and giant unilamellar vesicles (LUVs and GUVs, respectively). Surprisingly, in contrast to the behavior in living cells, all peptides readily entered the giant vesicles (>1 μm) as proved by confocal microscopy, while none of them could cross the membranes of LUVs (100 nm). For determination of the location of the peptides in the LUVs, a new concept was introduced, based on sensitive resonance energy transfer (RET) measurements of the enhanced fluorescence of acceptor fluorophores present solely in the inner leaflet. An easily adopted method to prepare such asymmetrically labeled liposomes is described. The membrane insertion depths of the tryptophan moieties of the peptides were determined by use of brominated lipids and found to be very similar for all of the peptides studied. We also demonstrate that infrared spectroscopy on the lipid carbonyl stretch vibration peak is a convenient technique to determine phospholipid concentration.

Keywords: Cell-penetrating peptide; Protein transduction domain; Energy transfer; Peptide topology; Tryptophan fluorescence; Liposome

1. Introduction

Due to their low plasma membrane permeability, the use of oligonucleotides and polypeptides for therapeutic purposes has generally been considered a distant goal. However, the identification of a number of cell-penetrating peptides (CPPs), which may mediate cytoplasmic delivery of large cargo molecules, has opened up new possibilities in biomedical research [1–3]. Among the most prominent CPPs are the HIV Tat peptides and penetratin, the latter

Abbreviations: BrPC, brominated phosphatidylcholine; CPP, cell-penetrating peptide; DA, distribution analysis; DIPEA, *N*,*N*-diisopropylethylamine; DFQP, depth-dependent fluorescence quenching profile; DOPC, 1,2-dioleoyl-*sn*-glycero-3-phosphocholine; DOPG, 1,2-dioleyol-*sn*-glycero-3-phosphoglycerol; 1, 2-dipalmitoyl-*sn*-glycero-3-phosphoserine; EDTA, ethylenediaminetetraacetic acid; eggPC, egg phosphatidylcholine; FAB-MS, fast atom bombardment mass spectrometry; FTIR, Fourier transform infrared spectroscopy; GUVs, giant unilamellar vesicles; HEPES, *N*-(2-hydroxyethyl)-piperazine-N′-(2-ethanesulfonic acid); HIV, human immunodeficiency virus; HPLC, high-performance liquid chromatography; LUVs, large unilamellar vesicles; lysoMC, *N*-(7-hydroxyl-4-methylcoumarin-3-acetyl)-1-palmitoyl-2-hydroxy-*sn*-glycero-3-phosphoethanolamine; lysoPE, 1-Palmitoyl-2-hydroxyl-*sn*-glycero-3-phosphoethanolamine; MCT, mercury cadmium tellur; MLVs, multilamellar vesicles; NBD-PE, *N*-(7-nitrobenz-2-oxa-1,3-diazol-4-yl)-1,2-dipalmitoyl-*sn*-glycero-3-phosphoethanolamine; OD, optical density; PA, phosphatidic acid; PC, phosphatidylcholine; PE, phosphatidylethanolamine; PI, phosphatidylinositol; PEG, poly(ethylene glycol); PM, parallax method; PM-IRRAS, polarization modulation infrared reflection absorption spectroscopy; POPC, 1-palmitoyl-2-oleoyl-*sn*-glycero-3-phosphocholine; POPG, 1-palmitoyl-2-oleoyl-*sn*-glycero-3-phosphoglycerol; RET, resonance energy transfer; ROI, region of interest; SbPC, soybean phosphatidylcholine; TOE, tryptophan octyl ester; UV, ultraviolet

* Corresponding author. Fax: +46 31 7723858.
E-mail address: danielp@phc.chalmers.se (D. Persson).

0005-2736/$ - see front matter © 2004 Elsevier B.V. All rights reserved.
doi:10.1016/j.bbamem.2004.07.008

derived from the Antennapedia homeodomain of *Drosophila*. These and other CPPs have been intensely studied the last decade in search for their mechanism of cellular entry. Until recently, these studies were almost invariably based on fluorescence microscopy on fixed cells and/or flow cytometry analysis [4–8]. Early work on penetratin suggested a receptor-independent and non-endocytotic cellular uptake, possibly involving interactions of the two tryptophans with the lipid matrix of the plasma membrane [9,10]. These conclusions were based on observations that cell internalization was neither hampered by incubation at low temperature nor by peptide modifications such as reversal of the amino acid sequence or introduction of three helix-breaking proline residues. On the other hand, substitution of the two tryptophans in the sequence drastically reduced the uptake. Also, studies of cell internalization of arginine-rich peptides have indicated that the arginines could be essential [8,11,12]. The reliability of these results is now in question, since two recent reports have shown that the use of post-incubation cell fixation causes serious artifacts in studies of cellular uptake of CPPs [13,14]. These often heavily positively charged peptides have a strong affinity for the plasma membrane and are not easily washed away. Upon cell fixation, peptide bound to the cell surface and also peptide taken up by endocytosis are redistributed, leading to misleading observations. Also, the strong propensity of these peptides to associate with the plasma membrane results in an overestimation of cellular uptake by flow cytometry.

The important discoveries first reported by Thorén et al. [15] demonstrated the need for new studies of cell internalization of CPPs. In a recent paper, we therefore examined the cellular uptake of penetratin as well as some analogs in live, unfixed cells. Contrary to earlier results from studies on fixed cells, we found that penetratin was internalized by endocytosis as was its tryptophan-substituted analog, Pen2W2F. Interestingly, an arginine-enriched analog, PenArg, was taken up both via endocytosis and another, apparently energy-independent, non-endocytotic pathway. A completely different behavior was observed for the analog where the arginines were exchanged for lysines. This peptide, PenLys, exhibited an astonishingly weak affinity for the plasma membrane and was not at all taken up by cells. It is noteworthy that although these results indicate an endocytotic uptake of penetratin, there are numerous studies in which membrane-impermeable compounds, when conjugated to penetratin, have exhibited the desired biological activity [16,17]. This suggests that, to an appreciable extent, the conjugates are able to escape the endosomes without extensive degradation. An indication of this was found in the observation that small amounts of peptide reached the nucleus in a significant fraction of the cells [15].

In the present work, we addressed the uptake of penetratin, PenArg, PenLys and Pen2W2F in large and giant unilamellar vesicles (LUVs and GUVs) in search of correlations between the cellular uptake of CPPs and their interactions with lipid bilayers. The results indicated, however, that whereas all peptides remained in the outer leaflet of LUVs, they easily traversed the membranes of GUVs. We also investigated the membrane insertion depths of the tryptophan residues in the peptides and found them to be very similar.

For the LUV penetration studies, we developed a new method for preparation of vesicles containing a lipid-linked probe only in the inner leaflet. Taking advantage of the vesicle exchangeability and slow flip-flop of lysolipids, we used easily prepared, micrometer-sized soybean phospholipid particles to extract exofacial probes from liposomes symmetrically labeled with the fluorescent lysolipid lysoMC. Rapid separation of particles from LUVs was achieved by centrifugation. The ability of the peptides to translocate across a LUV membrane was then assessed by measurements of resonance energy transfer (RET) from the tryptophans in the peptides to lysoMC residing in the inner leaflet of the membrane. The methodology introduced here for investigation of the topology of tryptophan-containing compounds in LUV membranes presents many advantages over existing methods. It should, in addition, be easily implemented for other RET donor–acceptor pairs and even for applications other than RET measurements. Furthermore, we demonstrated that infrared spectroscopy on the lipid carbonyl bond stretch vibration is a rapid and reliable technique to determine phospholipid concentration.

2. Materials and methods

2.1. Materials

1,2-Dioleoyl-*sn*-glycero-3-phosphocholine (DOPC) and egg phosphatidylcholine (eggPC) were purchased from Larodan. 1,2-Dioleyol-*sn*-glycero-3-phosphoglycerol (DOPG), tryptophan octyl ester (TOE) and HEPES were obtained from Sigma. EDTA (titriplex III) was purchased from Merck. Soybean phosphatidylcholine (Epikuron 200 SbPC) was a kind gift from Lucas Meyer and soybean lecithin (a polar lipid extract containing 45.7% PC, 22.1% PE, 18.4% PI, 6.9% PA and 6.9% other lipids) as well as 1-palmitoyl-2-stearoyl(6–7)dibromo-*sn*-glycero-3-phosphocholine, 1-palmitoyl-2-stearoyl(9–10)dibromo-*sn*-glycero-3-phosphocholine and 1-palmitoyl-2-stearoyl(11–12)dibromo-*sn*-glycero-3-phosphocholine ((6,7)-, (9,10)-, and (11,12)-BrPC, respectively) were purchased from Avanti Polar Lipids. *N*-(7-Nitrobenz-2-oxa-1,3-diazol-4-yl)-1,2-dipalmitoyl-*sn*-glycero-3-phospho-ethanolamine (NBD-PE) was obtained from Molecular Probes and Ac-18A-NH_2 was purchased from KJ Ross Pedersen AS. The oligonucleotide 5′GTAGATCACTGTAGTA-CACT3′, fluorescein-labeled at the 5′ end, was purchased from Eurogentec.

The buffer used in LUV experiments was 10 mM HEPES, 5 mM NaOH, 1 mM EDTA and 0.1 M NaCl (pH

7.4) and the buffer used in GUV experiments was 5 mM Tris, 10 mM K_3PO_4, 10 mM KH_2PO_4, 90 mM KCl, 1 mM $MgSO_4$, 0.5 mM EDTA, 1 mM NaN_3, pH 8.1. Deionised water from a Milli-Q system (Millipore) was used.

2.2. Peptide synthesis

Penetratin (RQIKIWFQNRRMKWKK), PenArg (RQIRIWFQNRRMRWRR), PenLys (KQIKIWFQNKKMKWKK) and Pen2W2F (RQIKIFFQNRRMKFKK) were synthesized as described previously [18], with amidated carboxyl termini. Peptides used in LUV experiments were acetylated at the amino terminus whereas peptides used in GUV experiments were labeled with 5-(and 6-)carboxyfluorescein at the amino terminus.

2.3. Synthesis and purification of lysoMC

LysoMC was synthesized by reacting 7-hydroxy-4-methylcoumarin-3-acetyl-succinimidyl ester (Molecular Probes) with 1-palmitoyl-2-hydroxyl-*sn*-glycero-3-phosphoethanolamine (lysoPE, Alexis). Twenty milligrams of the probe was incubated with two equivalents of DIPEA and 20 mg of the lysolipid in 1.8-ml methanol in an Eppendorf tube for 24 h at room temperature. The reaction mixture was then applied to a preparative reversed-phase HPLC (Kromasil C8 column, Eka Chemicals), and the product eluted with a 40-min gradient of 5–70% acetonitrile in acetate buffer (pH 6). The identity of the fluorescently labeled lipid was confirmed by FAB-MS and the purity further confirmed by analytical thin-layer chromatography. After purification, the product was lyophilized and stored at −20 °C. The reaction yield was approximately 60% with respect to lysoPE. For preparation of lysoMC-labeled vesicles, a stock solution of lysoMC dissolved in chloroform containing 1% methanol was used.

2.4. Preparation of LUVs

Large unilamellar vesicles (LUVs) of four different lipid compositions were used in this study. These four were DOPC/DOPG (molar ratio 60:40), eggPC/DOPG (60:40), pure DOPG and a soybean polar lipid extract. A dry lipid film was prepared from chloroform solutions of the lipids with or without 1 mol% lysoMC by removing the solvent on a rotary evaporator. The lipid film was placed in high vacuum for 2 h to remove trace amounts of chloroform. Vesicles were prepared by dispersion of the lipids in buffer by vigorous vortexing. The multilamellar vesicles (MLVs) were subjected to five freeze–thaw cycles before extrusion 21 times through two 100-nm polycarbonate filters on a LiposoFast-Pneumatic extruder (Avestin) to obtain LUVs.

2.5. Spectroscopic experiments

All fluorescence spectroscopy measurements were carried out on a Spex Fluorolog τ-3 spectrofluorometer (JY Horiba) using a 1×1-cm quartz cell thermostated at 25 °C. Peptide and TOE concentrations were determined from the UV absorbance measured on a Cary 4B UV–Vis spectrometer, using a ε_{280} for Trp of 5690 M^{-1} cm^{-1} [19].

2.6. Preparation of lipid particle suspensions

After suspension of dry SbPC lipid (20 mg/ml) by heavy vortexing, 1.5-ml samples were centrifuged in 2-ml Eppendorf tubes at 25 °C on a Heraeus Biofuge 28 RS with a 3740 rotor, applying the longest acceleration and braking times. The first centrifugation after vortexing was made at 5000×*g* for 5 min, while the subsequent ones were made at 50 000×*g* for 15 min. α-Tocopherol fluorescence was measured by exciting the sample at 290 nm and collecting the emission at 335 nm.

2.7. Preparation of vesicles asymmetrically labeled with lysoMC in the inner leaflet

Initially symmetrically labeled LUVs, 1.5 ml (total lipid concentration 2 mM), were added to a pellet of SbPC particles and the pellet was gently suspended. The sample was then allowed to stand for 15 min before it was centrifuged as described above at 50 000×*g* for 15 min. After centrifugation, the supernatant was removed and a small fraction of it was diluted with buffer to a volume of 2 ml in a cuvette. The fluorescence intensity at 400 nm upon excitation at 330 nm was then measured for 200 s before and 500 s directly after addition of an aliquot of 16.5 μl of 1 M NaOH, bringing the bulk pH to 11. The sudden increase in pH led to an instant drop in lysoMC fluorescence, followed by a slow, initially linear, decrease (data not shown), which probably reflects a slowly increasing intravesicular pH. By linear extrapolation, the intensity at the time of NaOH addition was determined and the induced drop in fluorescence after correction for background and the change in volume were calculated. The entire procedure was then repeated three or four times, and the pH-induced decreases in fluorescence intensity were compared to that obtained with symmetrically labeled LUVs, allowing determination of the amount of exofacial lysoMC after every washing step.

2.8. Resonance energy transfer

The method developed by Wimley and White [20] is based on quantification of RET by measurement of the quenching of Trp fluorescence. In quenching experiments, the experimental transfer efficiency (E) is defined as

$$E = 1 - \left(F_q/F_0\right) \quad (1)$$

where F_0 is the unquenched fluorescence intensity of the donor and F_q is the intensity in the presence of quencher. However, in the method developed here, using vesicles asymmetrically labeled with lysoMC in the inner leaflet, the better choice is to address the enhanced acceptor (lysoMC) fluorescence resulting from RET. Provided that the donor emission at the wavelength of detection of acceptor emission can first be subtracted, the experimental transfer efficiency is given by

$$E = \frac{\mathrm{OD_A}\left(\lambda_\mathrm{D}^\mathrm{ex}\right)}{\mathrm{OD_D}\left(\lambda_\mathrm{D}^\mathrm{ex}\right)}\left[\frac{F_\mathrm{AD}\left(\lambda_\mathrm{A}^\mathrm{em}\right)}{F_\mathrm{A}\left(\lambda_\mathrm{A}^\mathrm{em}\right)} - 1\right] \quad (2)$$

where $\mathrm{OD_A}(\lambda_\mathrm{D}^\mathrm{ex})$ and $\mathrm{OD_D}(\lambda_\mathrm{D}^\mathrm{ex})$ are the optical densities of the acceptor and donor at the donor excitation wavelength and $F_\mathrm{AD}(\lambda_\mathrm{A}^\mathrm{em})$ and $F_\mathrm{A}(\lambda_\mathrm{A}^\mathrm{em})$ are the acceptor emission intensities in the presence and absence of donor at an acceptor emission wavelength $\lambda_\mathrm{A}^\mathrm{em}$ [21]. However, due to difficulties in determining the exact concentrations of donor in the samples, we chose to report transfer efficiencies simply as enhancements of the acceptor fluorescence intensities and strived to keep the concentrations of both donor (Trp) and acceptor (lysoMC) constant. In general, though, the factor (corresponding to the first factor on the right-hand side of Eq. (2)) differentiating this value from E as it is defined in Eq. (2) was here ~0.7. The difficulties in achieving invariant donor concentrations in the samples stem from a strong propensity of the peptides [22], and also of TOE (data not shown), to adsorb to surfaces. This also gives an additional motivation for assessing the acceptor emission enhancement rather than the quenching of the donor.

2.9. RET experiments

Along the lines of Wimley and White [20], an excitation wavelength of 260 nm was used to maximize the $F_\mathrm{Trp}/F_\mathrm{lysoMC}$ ratio. Emission spectra were acquired between 300 and 500 nm and corrected for background. In RET experiments, the concentration of peptide and TOE was ~0.7μM with respect to Trp (the penetratin peptides contain two Trp) and the total lipid concentration was 100 μM. It was ascertained by titration with unlabeled vesicles [22] in separate experiments that at these concentrations, the Trp-containing compounds were completely bound to the vesicles. In order to obtain pure lysoMC spectra (Fig. 2B) from RET spectra (Fig. 2A), the spectrum of a peptide or TOE in unlabeled vesicles was multiplied by a factor estimated from the Trp contribution to the RET spectrum at the adequate λ_max(Trp) and was then subtracted from the RET spectrum.

In some experiments, lysoMC was added to the outer leaflet of LUVs. This was made by first drying a chloroform solution of lysoMC under a stream of nitrogen, after which the sample was placed in high vacuum to remove trace amounts of chloroform. The lysolipid was then dissolved in buffer (to 100 μM) by vortexing for 5 min. LysoMC has a high water solubility due to micelle formation, but is completely incorporated in vesicles when present [20]. Accordingly, when added to a dispersion of preformed liposomes, lysoMC rapidly partitioned into the outer leaflet. This could be followed by fluorescence measurements, since the emission spectrum changes from a unimodal character in micelles to a bimodal character in vesicles (see Results).

2.10. Flip-flop assay

In separate control experiments, it was checked that the membrane association of peptide or TOE does not result in lysoMC flip-flop across the vesicle membranes. First, a five times excess of LUVs containing 1 mol% NBD-PE was added to 50 μM vesicles symmetrically labeled with lysoMC. This led to a rapid decrease in the fluorescence intensity measured at 450 nm upon excitation at 330 nm, due to diffusion of exofacial lysoMC to the NBD-labeled liposomes where its fluorescence was quenched. After 5 min, when the fluorescence intensity had reached a constant value, peptide or TOE was added at concentrations three times higher than in the RET experiments, in order to obtain the same peptide to total lipid ratios (~1:285 for the penetratin peptides and ~1:143 for Ac-18A-NH_2) or TOE to total lipid ratio (~1:143) in these samples.

2.11. Quenching of tryptophan fluorescence by brominated lipids

Depth-dependent fluorescence quenching experiments of tryptophan were performed with LUVs composed of DOPC, DOPG, and either (6,7)-, (9,10)-, or (11,12)-BrPC at molar ratios of 30:40:30. BrPC concentrations were determined by Fourier transform infrared (FTIR) spectroscopy on the lipid carbonyl stretch vibrations (see below). LUVs were prepared as described in Section 2.4. Fluorescence intensities in the absence of quencher (F_0) were measured in DOPC/DOPG (60/40) vesicles. The excitation wavelength was set to 280 nm and emission spectra were recorded between 315 and 400 nm with an increment of 1 nm and an integration time of 2 s. All experiments were performed in a 1×1-cm quartz cuvette that was surface-modified with poly(ethylenimine) to minimize peptide adsorption to the cuvette walls [22]. The cuvette was filled with a 1% (w/v) solution of poly(ethylenimine) in deionised water and left for 30 min at room temperature and thereafter rinsed extensively with deionised water. The lipid concentration was 100 μM and peptide concentrations were ~0.7 μM. Emission spectra were corrected for background contributions and the total intensity was calculated as the sum of all measured intensities in each spectrum. Depth-dependent fluorescence quenching profiles (DFQPs) were fitted to data in Matlab

(Mathworks) using the distribution analysis (DA) method [24,25] as well as the parallax method (PM) [26–28]:

$$\text{DA:}\quad \ln\frac{F_0}{F(h)} = \frac{S}{\sigma\sqrt{2\pi}}\cdot\exp\left[-\frac{(h-h_m)^2}{2\sigma^2}\right] \tag{3}$$

$$\text{PM:}\quad \begin{aligned} \ln\frac{F_0}{F(h)} &= \pi\cdot C\cdot\left[R_c^2-(h-h_m)^2\right] && h-h_m<R_c \\ \ln\frac{F_0}{F(h)} &= 0 && h-h_m\geq R_c \end{aligned} \tag{4}$$

In these equations, F_0 is the fluorescence intensity in the absence of quencher whereas $F(h)$ is the intensity in the presence of quencher at the distance h (Å) from the bilayer center. h_m (Å) is the average insertion depth of the tryptophan residue. In DA, the DFQP data are fitted with a Gaussian function where σ denotes the dispersion, which is related to the distribution of the Trp chromophore, and S is the area under the profile, which is proportional to the quenchability of the Trp moiety. In the parallax method, data are fitted with a truncated parabola, and R_c is the radius of quenching [29,30]. Even though the brominated lipids used contain no double bonds, they form bilayers of apparently equal thickness to POPC [31], with a hydrocarbon core of ~29 Å and a total bilayer thickness of ~49 Å. The brominated lipids have properties similar to lipids with one monounsaturated acyl chain since the bulkiness of the bromine atoms has comparable effects on lipid packing to a *cis* double bond [32]. According to Wiener and White [33], DOPC bilayers have a hydrocarbon core of approximately 30 Å. It is therefore reasonable to assume that the average bromine distances from the lipid bilayer center, as determined by McIntosh and Holloway [31], are valid also in the vesicles used in this study. Average bromine distances from the bilayer center (h) were thus taken as 11.0, 8.3, and 6.5 Å for (6,7)-BrPC, (9,10)-BrPC, and (11,12)-BrPC, respectively.

2.12. Lipid stock solution concentration determinations

In order to prepare LUVs containing equal amounts of brominated lipids, stock solution concentrations were determined by FTIR spectroscopy on the carbonyl stretch vibration and the results were compared with colorimetric concentration determinations using Stewart assay. The results were related to those obtained for a DOPC solution, the exact concentration of which was determined by weighing of dry lipid. FTIR measurements were performed on a Bruker IFS 66v/S FTIR spectrometer equipped with a nitrogen-cooled MCT-detector. A sample cell with sodium chloride windows and a path length of 0.2 mm was used. All measurements were performed on chloroform solutions and spectra were corrected for chloroform background contributions. Concentrations were determined by integrating the peak at 1740 cm^{-1}, corresponding to the carbonyl stretch vibration. Stewart assay was used as follows [34]: Briefly, 700-μl lipid stock solution was mixed with 700-μl Stewart assay reagent (0.1 M ammonium ferrothiocyanate) in an Eppendorf tube. The samples were vortexed for 2 min followed by 3 min of centrifugation at 8500 rpm. Five-hundred microliters of the chloroform phase was transferred to a 1×1-cm quartz cell and diluted five times. The optical density (OD) was measured on a Cary 4B UV–Vis spectrometer at 485 nm.

2.13. Preparation of GUVs

GUVs were prepared by a dehydration/rehydration method [35,36] from a polar lipid extract of soybean lecithin (Avanti Polar Lipids), consisting of a mixture of PC (45,7%), PE (22,1%), PI (18,4%), PA (6,9%) and others (6,9%). Briefly, a dry phospholipid film was prepared by rotary evaporation of a chloroform solution of lipid. The lipid film was swelled by careful addition of buffer solution (5 mM Tris, 10 mM K_3PO_4, 10 mM KH_2PO_4, 90 mM KCl, 1 mM $MgSO_4$, 0.5 mM EDTA, 1 mM NaN_3, pH 8.1) and left in a refrigerator overnight. Glycerol (1% v/v) was added to the solution, which was then placed in an ultrasonic bath for 15 min. Five microliters of the resulting lipid dispersion (1 mg/ml) was placed on a coverslip glass and the solution was dehydrated in a vacuum desiccator for 20 min. The dry lipid film was rehydrated with 0.5-ml buffer to swell the film. MLVs as well as GUVs were formed within minutes.

2.14. Confocal laser scanning microscopy

Peptide translocation across GUV membranes was assessed using a laser scanning confocal unit (MRC1024, Bio-Rad) mounted on the side port of an inverted microscope (TE-300, Nikon). The dyes used in the experiment (carboxyfluorescein and fluorescein) were excited using a fibre-coupled Ar laser (488 nm). The samples were imaged using a 40′ Plan Fluor objective (Nikon) with a numerical aperture of 0.75. In combination with the applied confocal pinhole, this resulted in a depth of field (or longitudinal resolution) of 2 μm. A 522DF35 filter (emission 505–540 nm) was used. The signal was collected by using a five-frame Kalman collection filter. Relative fluorescence was measured using LaserPix software (Bio-Rad).

3. Results

3.1. RET spectroscopy

A spectroscopic characterization of the lysolipid probe lysoMC and the properties of the RET donor–acceptor pair tryptophan-lysoMC has been done earlier by Wimley and White [20]. The absorbance of lysoMC with a maximum at 335 nm (ε=14950 M^{-1} cm^{-1}) gives a good spectral overlap with the fluorescence emission of membrane-associated

tryptophans, resulting in efficient RET with a Förster distance, R_0, of ~25 Å.

Wimley and White [20] recently introduced a method for determination of membrane topology of Trp-containing compounds, based on quantification of RET by measurement of the quenching of Trp fluorescence. The evaluation of the topology relies on a comparison of the quenching efficiencies in vesicles symmetrically labeled with lysoMC and in vesicles containing lysoMC only in the outer leaflet. However, the method for preparation of vesicles containing lysoMC only in the inner leaflet that is presented here allows monitoring of translocation across the membranes by direct detection of enhanced lysoMC fluorescence. Although this requires consideration of both transbilayer RET and direct excitation of the acceptor, unambiguous data were obtained from relatively simple experiments (see below).

As seen in Fig. 1A, the emission spectrum of vesicle-associated lysoMC upon excitation at 330 nm (and at wavelengths down to at least 260 nm, data not shown) exhibits two bands with maxima at ~400 and ~460 nm at neutral pH. However, when titrating a dispersion of outer leaflet-labeled vesicles with NaOH to pH 11, the band at 400 nm disappears (Fig. 1A). If the pH instead is lowered, the 460-nm band decreases and a new band at ~495 nm is observed (data not shown). Thus, the two bands in the pH 7.4 spectrum probably correspond to the neutral (400 nm) and tautomer anion (460 nm) methylcoumarin species (Fig. 1B) in the excited singlet-state, whereas the band at 495 nm arises from the protonated species [37]. In the present study, the spectral change obtained upon increasing the pH to 11 was used to determine the amount of lysoMC in the exofacial leaflet of the vesicles (see below and Materials and methods).

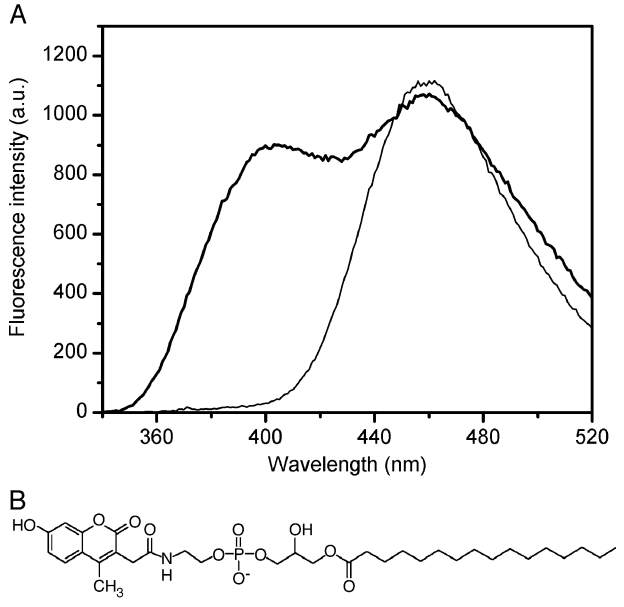

Fig. 1. (A) Fluorescence emission spectra of lysoMC (0.5 mol%) in the outer leaflet of DOPC/DOPG (60:40) LUVs (100 μM) at pH 7.4 (thick line) and pH 11 (thin line). The sample was excited at 330 nm. (B) Chemical structure of lysoMC, with the methylcoumarin moiety in its neutral form.

3.2. Preparation of vesicles containing lysoMC in the inner leaflet

For assessment of the ability of the penetratin peptides to translocate across the membranes of LUVs, we developed a method for preparation of liposomes labeled with the fluorescent lysolipid lysoMC in the inner leaflet. This was accomplished by making use of the fact that lysoMC is readily exchangeable between vesicles and also between other lipidic structures [20] and that lysolipid transbilayer exchange (flip-flop) is slow [38]. Thus, repeated "washing" of initially symmetrically labeled vesicles with lipid particles and, in between, centrifugation of the sample resulted in vesicles with a negligible amount of lysoMC in the outer leaflet. Importantly, the amount of fluorescent probe remaining in the outer monolayer of the vesicles could be determined after every washing step.

First, a suspension of lipid particles was prepared by 10 min of heavy vortexing of dry lipid (Epikuron 200 SbPC, see Materials and methods for further details in the procedures described below) in buffer followed by a number of centrifugation steps. The vortexed sample was observed in a microscope and found to contain both lipid particles with undefined structure, mostly of sizes between 5 and 20 μm, and MLVs generally somewhat smaller in size. The first centrifugation was made at a moderate speed ($5000\times g$) in order to retain smaller lipid structures in the supernatant, which was then removed. The resulting pellet was then resuspended in fresh buffer by gentle mixing with a pipette. The procedure was then repeated four times, but with centrifugation at $50\,000\times g$. Ideally, the supernatant after centrifugation should be free from remainders of SbPC before the pellet was suspended in a lysoMC LUV dispersion. This could be checked by measuring the fluorescence of α-tocopherol, which is present in small amounts in Epikuron 200. Whereas the concentration of α-tocopherol in the supernatant of the first centrifugation was 1% of that of the suspended sample, only ~0.05% remained after the fifth centrifugation. These estimates of lipid concentrations were in excellent agreement with control experiments using the Stewart assay [34] (data not shown).

The pellets of lipid particles could now be used for washing LUVs symmetrically labeled with lysoMC. Thus, a dispersion of such LUVs was added to a pellet after the supernatant had been removed and the pellet was gently suspended with a pipette. The proportions of SbPC and LUV lipid were ~13:1. The sample was allowed to stand for 15 min to give the lysoMC time to equilibrate between the LUVs and the SbPC particles, and was then centrifuged for 15 min at $50\,000\times g$. The LUV supernatant was then carefully removed with a pipette and the amount of lysoMC remaining in the outer leaflet was assessed. This was done by utilizing the pH dependence of the lysoMC fluorescence

(see above). Upon addition of NaOH, the emission at 400 nm of the lysoMC residing in the outer leaflet is almost eliminated, whereas the fluorescence of the lysoMC in the inner leaflet is initially unaltered (see Materials and methods). Typical examples of estimates of the fraction of exofacial lysoMC remaining after five subsequent washings were 14.0%, 3.4%, 1.6%, 1.1% and 1.0%. Additional washing steps did not further improve the result, suggesting either that a certain extent of lysoMC flip-flop is induced by, e.g., centrifugation or that there is an inherent discrepancy in the method applied for quantification of exofacial lysoMC. However, as will be shown below, a potential lysoMC remainder of only 1% in the outer leaflet has no significant bearing on the RET experiments. In this context, it is noteworthy that both the lysoMC flip-flop rate and the lysoMC asymmetry in the nominally symmetrical LUVs could be estimated using the "pH shock" method. LysoMC LUVs that had been washed five times were used for RET experiments within, at most, 4 h. After 6 h, measurements indicated an exofacial lysoMC population of 2–2.5% of that prevailing before the first washing step, showing that lysoMC flip-flop is indeed slow and certainly negligible for the experiments performed in this study (see below). Furthermore, the decrease in fluorescence of symmetrically labeled lysoMC at the instant pH change suggested that ~59% of the lysoMC resided in the outer leaflet of these LUVs. This is somewhat more than what would be expected (~54%) from simple geometrical calculations of lipid distribution in 100-nm liposomes assuming a bilayer thickness of 4 nm. Possibly, this reflects a preference of lysoMC for the outer leaflet due to its conical shape and the positive curvature of the outer bilayer.

3.3. Translocation across the membranes of LUVs

Vesicles containing lysoMC only in the inner leaflet were used to determine whether penetratin and its analogs PenArg and PenLys, upon binding to LUV membranes, were able to translocate across the lipid bilayer. Included also in the study were TOE and the 18-residue amphipathic helix peptide Ac-18A-NH_2 [39] as reference compounds. TOE was previously shown by Wimley and White [20] to equilibrate across the membranes of POPG and POPC LUVs, whereas Ac-18A-NH_2 in the same study remained in the outer leaflet.

Fluorescence spectra were acquired before and after addition of peptide or TOE to LUVs asymmetrically labeled with lysoMC in the inner bilayer. From the spectra in Fig. 2A, it can be concluded that the Trp of TOE, Ac-18A-NH_2 and penetratin, although to different extents, exhibit resonance energy transfer to the lysoMC residing in the inner leaflet. This is most evident in the region around 460 nm where there is a noticeable increase in intensity, despite the fact that Trp fluorescence is here negligible. The result is even more tangible when the Trp fluorescence of each compound, as described in Materials and methods, is subtracted from the spectrum (Fig. 2B). Clearly, the enhancement in lysoMC fluorescence observed for the membrane-translocating TOE is many times larger than for both penetratin and the negative reference peptide Ac-18A-NH_2. In Table 1, the relative increases in lysoMC emission at 460 nm upon introduction of peptide are summarized for DOPC/DOPG (60/40) LUVs. Both PenArg and PenLys gave results very similar to those obtained for Ac-18A-NH_2 and penetratin, indicating that none of the peptides was able to reach the inner leaflet. The experiments were repeated for LUVs with three other lipid compositions (eggPC/DOPG (60:40), pure DOPG and the soybean polar lipid extract used in the GUV study; see below), and for all three, results very similar to those presented for DOPC/DOPG vesicles were obtained.

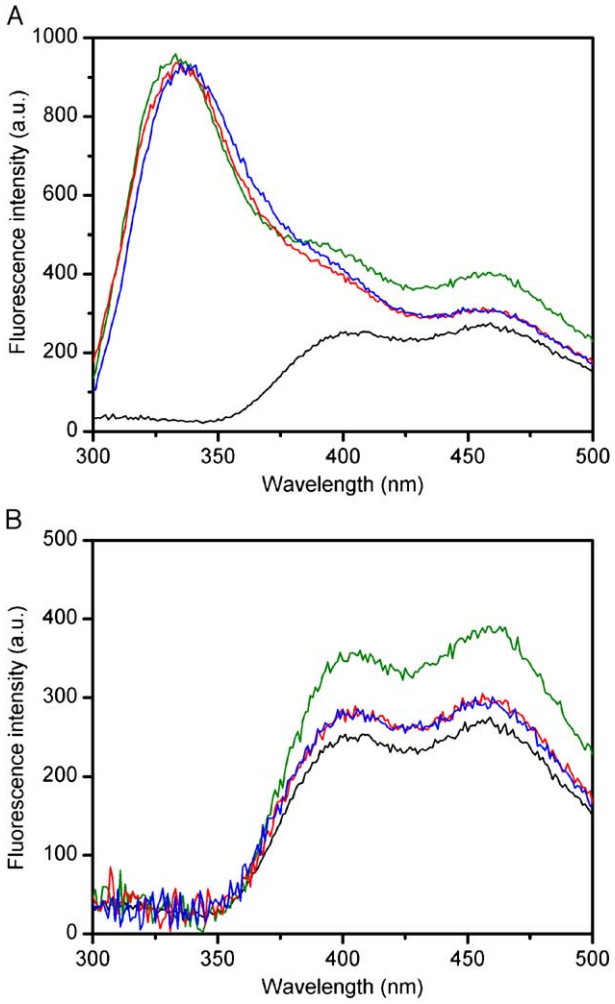

Fig. 2. (A) Fluorescence emission spectra upon excitation at 260 nm of DOPC/DOPG (60:40) LUVs (100 μM) with lysoMC in the inner leaflet, in the absence (black) and in the presence of TOE (green), Ac-18A-NH_2 (red) or penetratin (blue). Tryptophan concentrations were ~0.7 μM. (B) Fluorescence emission spectra of DOPC/DOPG (60:40) LUVs (100 μM) with lysoMC in the inner leaflet, in the absence (black) and in the presence of TOE (green), Ac-18A-NH_2 (red) or penetratin (blue) with the tryptophan emission contributions subtracted (see Materials and methods).

Although less efficient than in the case of TOE, there was clearly RET (~10%) also from the peptides to lysoMC. The

Table 1
Summary of the determination of translocation across the membranes of DOPC/DOPG (60:40) LUVs

Compound	λ_{max} (nm)[a]	RET (%)[b]
Tryptophan octyl ester (TOE)	333	44.9
Ac-18A-NH_2	334	11.5
Penetratin	336	9.9
PenArg	335	12.0
PenLys	335	10.0

[a] Wavelength of fluorescence emission maximum.
[b] Resonance energy transfer to lysoMC in the inner LUV leaflet, expressed as relative enhancement of lysoMC fluorescence at 460 nm. The experimental uncertainties are in the range of 2% to 3%. In LUVs containing lysoMC solely in the outer leaflet, the RET values were in the range 45–55% for all compounds (see text).

origin of this was addressed by adding defined amounts of lysoMC to the outer leaflets of LUVs in which the exofacial lysoMC had been washed away. RET experiments with these liposomes showed that an addition of lysoMC corresponding to an exofacial population of 5% of the population in symmetrically labeled vesicles was required to achieve a measurable increase in the enhancement of lysoMC fluorescence. This provides evidence that the lysoMC remaining in the outer leaflet after washing has no influence on the RET experiments and that the enhanced lysoMC emission in the peptide experiments stems from transbilayer RET. In order to confirm that the peptides stay in the outer bilayer, we also studied RET in DOPC/DOPG LUVs labeled with lysoMC only in the outer leaflet. Indeed, in these experiments, where care was taken to prepare samples with the same concentrations of both peptides and lipids as in the experiments on inner leaflet-labeled LUVs (see Materials and methods), the increase in lysoMC fluorescence was in the range of 45% to 55% for all compounds.

Certainly, RET experiments on Trp-containing compounds interacting with asymmetrically labeled vesicles require that this interaction does not result in flip-flop of the lipid probe. In this study, this was checked in separate experiments where an excess of NBD-labeled vesicles was added to lysoMC LUVs (see Materials and methods). Since lysoMC is readily exchangeable between vesicles and is quenched by NBD, exofacial lysoMC will diffuse to the NBD-labeled liposomes and the fluorescence will decrease [20]. In no case did the addition of peptide or TOE to a mixture of lysoMC and NBD vesicles induce a decrease in lysoMC fluorescence (data not shown), showing that induced lysoMC flip-flop did not occur in our experiments.

3.4. Determination of the membrane insertion depth of Trp

The membrane insertion depth of the tryptophan residues in penetratin, PenArg, and PenLys, TOE and Ac-18A-NH_2 was investigated using LUVs. The cationic hemolytica peptide melittin was used as an additional reference compound. Depth-dependent fluorescence quenching data are presented in Table 2 as percentages of the total

Table 2
Quenching efficiencies ($F(h)/F_0$)[a] in percent

	Penetratin	PenArg	PenLys	TOE	Ac-18A-NH_2
DOPC/DOPG	100	100	100	100	100
(6,7)-BrPC	64	61	61	73	63
(9,10)-BrPC	69	64	65	72	69
(11,12)-BrPC	83	78	78	87	82

[a] F(h) is the tryptophan fluorescence intensity in the presence of quenchers at the distance h from the bilayer center, and F_0 is the tryptophan fluorescence intensity in the absence of quencher measured in DOPC/DOPG (60:40) vesicles.

fluorescence intensity in DOPC/DOPG (60:40) vesicles. All investigated peptides exhibit comparable quenching patterns with most pronounced quenching in (6,7)-BrPC vesicles, whereas TOE shows similar degrees of quenching in (6,7)- and (9,10)-vesicles. Table 3 shows the average membrane insertion depth (h_m) presented as the distance from the bilayer center of the Trp residues in each peptide, derived with distribution analysis (DA) or the parallax method (PM) (see Materials and methods). Also presented in Table 3 are the fitting parameters for both methods. Fig. 3 illustrates the fitting to data of the depth-dependent quenching profiles for penetratin, calculated with DA and PM. For all peptides, the difference in the Trp insertion depth determined with the two methods is less than 1 Å. All investigated peptides have an average Trp insertion depth of 10–11 Å, whereas the Trp moiety in TOE seems to be inserted somewhat deeper. Fitting DFQPs to melittin quenching data (data not shown) with DA and PM yielded average membrane insertion depths of 10.2 and 10.9 Å, respectively.

3.5. Determination of lipid concentration by FTIR spectroscopy

BrPC concentrations determined by FTIR and Stewart assay are reported in Table 4. The concentrations are averages of three independent measurements and the standard deviation (S.D.) is reported for each data point. The

Table 3
Average insertion depths as determined by the distribution analysis and parallax methods

Compound	DA			PM-2	
	h_m (Å)[a]	σ (Å)[b]	S[c]	h_m (Å)[a]	R_c (Å)[d]
Penetratin	10.2	2.7	3.2	10.9	5.8
PenArg	9.9	2.8	3.8	10.8	6.2
PenLys	10.1	3.0	3.9	10.8	6.1
TOE	9.6	2.1	2.1	10.2	5.0
Ac-18A-NH_2	10.3	2.9	3.5	10.9	5.9

[a] h_m is the average insertion depth, measured as the distance from the bilayer center.
[b] σ is the dispersion which is related to the membrane distribution of the Trp chromophore.
[c] S is the area under the quenching profile, which is proportional to the quenchibility of the Trp residue.
[d] R_c is the radius of quenching, defining the size of a circle centered around the Trp moiety outside which no quenching should occur.

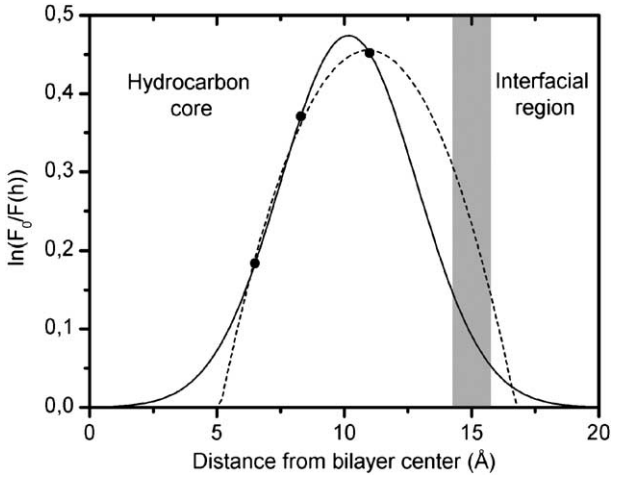

Fig. 3. Depth-dependent quenching profiles of penetratin, fitted to data using the distribution analysis (solid line) and the parallax method (dashed line). The gray line marks the boundary between the hydrocarbon core and interfacial region.

expected concentrations, as stated by the manufacturer (Avanti Polar lipids), were 2.5 mg/ml (after four times dilution) for all three types of brominated phospholipids. It can thus be concluded that all concentrations are well above the stated, and that there is a significant difference in concentration between (6,7)-, (9,10)-, and (11,12)-BrPC. The Stewart assay and the FTIR measurements provide very similar results, although the standard deviations are considerably larger in the Stewart assay.

3.6. Translocation across the membranes of GUVs

The study of penetratin, PenArg and PenLys in LUVs indicated that the peptides remained in the outer leaflet of such vesicles upon association. However, we have previously shown that penetratin translocates across the membranes of GUVs [18]. We therefore performed an extension of that study to address the membrane translocation abilities of PenArg and PenLys. Included in the experiments also was Pen2W2F, a penetratin peptide where the tryptophans have been exchanged for phenylalanines. The vesicular samples were prepared by a dehydration/rehydration method that has previously been shown to produce a mixture of MLVs and GUVs [35,36]. The unilamellar vesicles obtained by this method are typically 1–300 μm in diameter [36].

Table 4
Comparison of brominated phospholipid concentrations as determined by FTIR measurements and Stewart assay

Lipid	FTIR		Stewart assay	
	[mg/ml]	S.D.[a]	[mg/ml]	S.D.[a]
(6,7)-BrPC	2.75	0.036	2.83	0.048
(9,10)-BrPC	3.10	0.017	3.00	0.036
(11,12)-BrPC	2.96	0.032	2.94	0.060

[a] S.D.=standard deviation.

Upon hydration with 0.5-ml buffer of the lipid film dried in on a coverslip (see Materials and methods), MLVs and GUVs were formed within minutes. Most of the GUVs were attached directly or via other GUVs to an MLV. However, several freestanding GUVs were also found. After 15 min, which was more than sufficient time for the sample to settle, a small volume of peptide solution was very carefully added (final concentration ~6 μM) at the top of the droplet. After an additional 10–15 min, the peptide had diffused down to the vesicles sitting on the coverslip and the evolution of the peptide distribution could be followed in a confocal laser scanning microscope. In Fig. 4 is displayed the evolution with time of the fluorescence (on a scale from 0 to 255 arbitrary units, where the background intensity is ~10) in defined "Regions of interest" (ROI) in a sample to which penetratin had been added. ROI 2 was positioned in a freestanding GUV and ROI 3 in an MLV, whereas ROI 1 was placed in the surrounding buffer solution. The measured intensities show that the peptide has a strong affinity for MLVs, but also that the fluorescence inside the GUV follows closely that of the surrounding buffer. This indicates

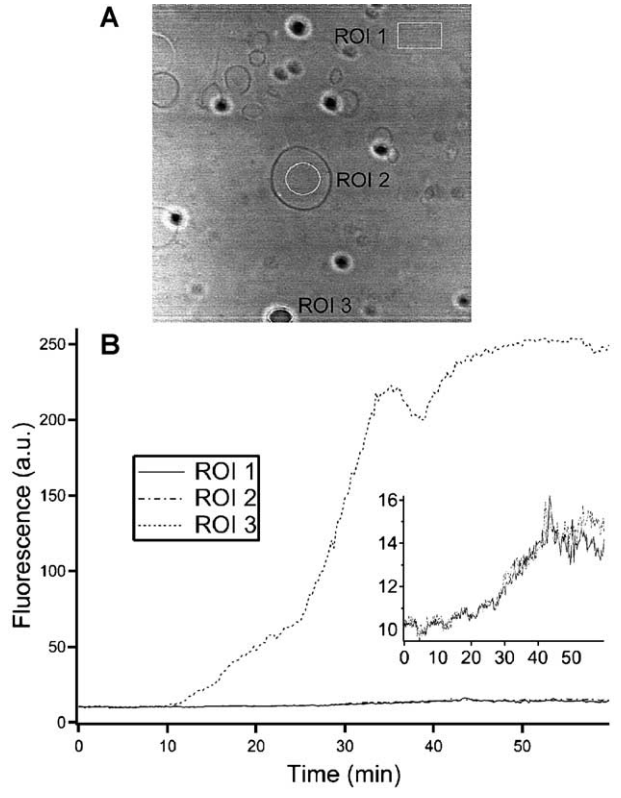

Fig. 4. Confocal laser scanning microscopy analysis of the distribution of carboxyfluorescein-labeled penetratin after addition to a sample of MLVs and GUVs sitting on a coverslip. (A) Bright-field image indicating the "Regions of interest" (ROI) for which the fluorescence intensity evolution with time is displayed in B. ROI 1 is positioned in buffer solution, ROI 2 in a freestanding GUV and ROI 3 encloses an MLV. (B) Fluorescence intensity (on a scale from 0 to 255 arbitrary units, where the background intensity is ~10) as a function of time in the ROIs indicated in A. Peptide was added at the top of the droplet at time 0. The inset displays the time evolution of the fluorescence in only ROI 1 and ROI 2.

that the peptide is indeed able to rapidly translocate across the GUV membrane. Very similar results were obtained also for the other three peptides (data not shown), implying that there is no marked difference between them in the ability to traverse GUV membranes. To obtain more data, images were taken on several locations in the samples and line profiles of the fluorescence intensities were constructed. One such line profile, which is representative of the results obtained for all four peptides, is displayed in Fig. 5A for PenArg and it exhibits the strong affinity of the peptide for negatively charged lipid bilayers, a common property of the penetratin peptides [40]. It also shows that the fluorescence intensity contributions from inside and outside the vesicles are roughly the same.

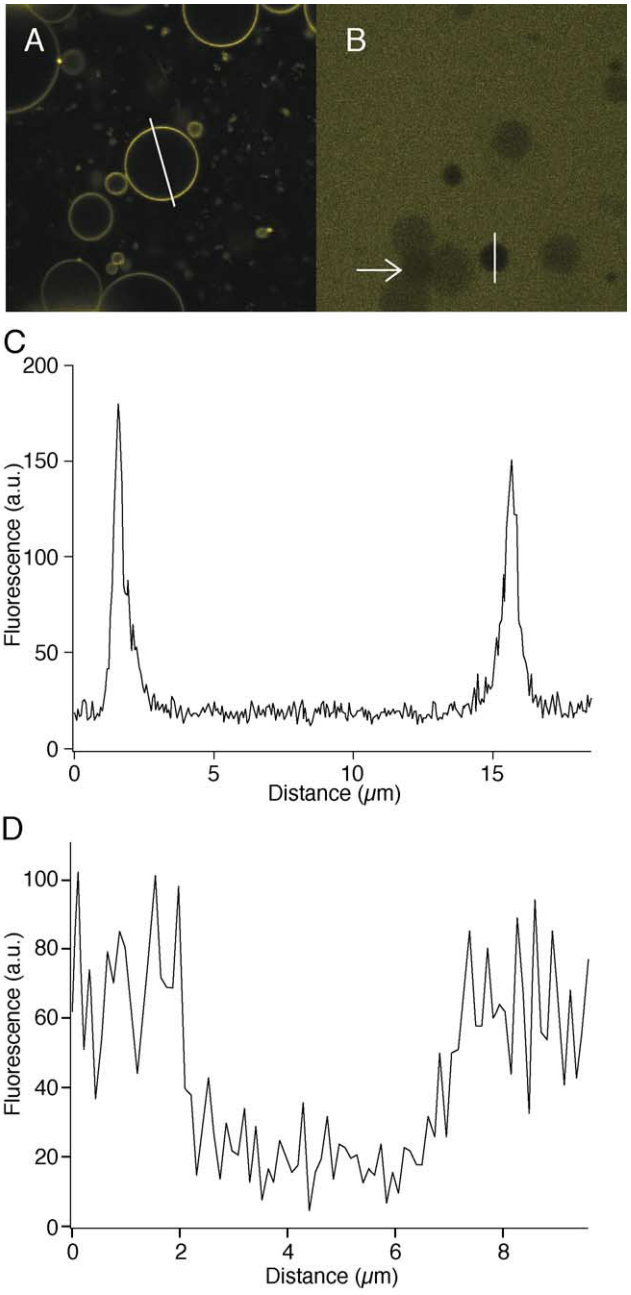

Fig. 5. Confocal laser scanning microscopy images of the distribution of (A) carboxyfluorescein-labeled PenArg and (B) a fluorescein-labeled 20-mer oligonucleotide in vesicle samples. (A) A line profile of the fluorescence intensity, indicated by the white line through a free-standing GUV, is displayed in C. (B) A line profile of the fluorescence intensity, indicated by the white line through a free-standing GUV, is displayed in D. The white arrow points at an MLV with three GUVs attached to it.

In control experiments using photobleaching, we verified that the fluorescence intensity increase observed inside the GUVs was not due to artifactual stray light emanating from the intensely fluorescent membranes. This could have been suspected, since GUVs sitting on the surface are expected to have profiles like slightly flattened spheres. Thus, with the focal plane located in the mid-section of the vesicle, maximum laser intensity was applied for 30 s resulting in strongly reduced fluorescence. The fluorescence was, however, recovered within minutes. Although this is an indication of the presence of peptide inside the GUVs, the range of the photobleaching in the longitudinal direction needed to be addressed. A supplementary experiment was therefore performed. The focal plane was moved to the level of the membrane facing the buffer solution and the intensity was measured before moving the focal plane down to the mid-section of the vesicle. Upon photobleaching of this section, the focal plane was rapidly brought back to the membrane level where the fluorescence intensity was measured again. No effect on the fluorescence in the membrane was detectable. All in all, this is strong evidence that peptide is present in the GUVs at concentrations comparable to that in the surrounding buffer.

Supplementary experiments with a fluorescently labeled 20-mer oligonucleotide were performed to assess the integrity of the GUV membranes. As in the peptide experiments, the fluorescence in MLVs and GUVs was examined upon addition of the analyte at the top of the droplet. As the oligonucleotide did not bind to the lipid structures, the buffer solution exhibited a strong and uniform fluorescence (Fig. 5B). Interestingly, large differences in permeability were observed for the vesicles. MLVs as well as GUVs directly associated with an MLV were apparently completely permeable to the oligonucleotide, since a uniform internal fluorescence intensity comparable to that of the buffer was obtained. Freestanding GUVs, on the other hand, were generally much more impermeable, as manifested by a substantially weaker interior fluorescence (Fig. 5B).

4. Discussion

Clearly, experiments based on RET from tryptophans to lysoMC residing in the inner leaflet of asymmetrically labeled liposomes allow unambiguous determination of the location of tryptophan-containing compounds. The inner leaflet-labeled lysoMC vesicles are easily prepared by the method introduced here. A similar approach has been applied before [41], using GUVs to wash away exofacial lipid-linked probes from smaller-sized vesicles.

However, the lipid particles used here as sinks for lysoMC are considerably easier to prepare, especially in the amounts required for experiments such as those performed in this work. The use of lysolipids instead of diacyl lipids in the preparation of vesicles asymmetrically labeled with a lipid probe presents a number of advantages [20]. Lysolipids are easier to handle since they are "soluble" in aqueous solutions in micellar form, but rapidly partitions into lipid vesicles. In the case of diacyl lipids, asymmetric vesicles are often prepared by dilution of an organic solution of lipid probes into a vesicle dispersion [42]. However, this often leads to incomplete incorporation of the diacyl probe due to rapid precipitation [20]. Furthermore, due to the very slow vesicle exchange rates of diacyl lipids [43,44], inner leaflet-labeled vesicles are not possible to prepare by a method like that presented in this work, but require chemical modification of exofacially located probes in symmetrically labeled vesicles [45] or the use of exchange proteins [46].

The results obtained in the experiments on inner leaflet-labeled LUVs demonstrated substantially more efficient resonance energy transfer from TOE than from peptides to the endofacial lysoMC (Table 1). Taken together with the indications of a similar membrane depth of the tryptophans of all compounds under investigation (see Table 3), this provides evidence for the conclusion that whereas TOE readily equilibrates across the bilayer, the peptides remain in the outer leaflet. Moreover, while the lysoMC fluorescence was equally enhanced by RET from TOE in both inner and outer leaflet-labeled vesicles, the energy transfer from all peptides was several times more efficient to exofacial than to endofacial lysoMC. The fact that the enhancement of lysoMC fluorescence obtained with TOE, in both kinds of vesicles, is in level with that obtained for the peptides in outer leaflet-labeled LUVs is, however, surprising. Since TOE is distributed to both sides of the membrane and the transbilayer RET is relatively inefficient, a significantly smaller enhancement was expected. The reason for this discrepancy is not known, but it might reflect a different orientation in the membrane of the TOE and the peptide tryptophans relative to the methylcoumarin chromophore [47]. In this context, it is also noticeable that the differences in spectral overlap [21] of the emission spectra of the Trp-containing moieties, with the absorption spectrum of lysoMC (ε_{max} at 335 nm) due to their variously blue-shifted emission (see Table 1), seem negligible since no correlation with RET efficiency could be detected.

Wimley and White [20] previously assessed the topology of membrane-associated, tryptophan-containing compounds by comparing the quenching efficiencies in vesicles containing lysoMC in either the outer or in both leaflets. In RET experiments using inner leaflet-labeled vesicles, however, the enhanced acceptor fluorescence was found to be a far more sensitive and reliable tool. This applies in particular to studies of compounds with a strong tendency to adsorb to surfaces, as was the case in this work. Even relatively small variations in donor concentration in the samples will lead to a large variability in the experimental quenching efficiencies, as these are only a few percent in cases of pure transbilayer RET and are directly affected by concentration differences. The enhanced acceptor fluorescence, on the other hand, is much more stable, since it is roughly proportional to the actual donor concentration (data not shown).

Our result for penetratin in LUVs is in agreement with a recent study by Drin et al. [48], who reported that penetratin remains in the outer leaflet of POPC/POPG LUVs upon association. The translocation assay used in that work was, however, different in that it was based on tryptophan quenching in vesicles symmetrically labeled with 15 mol% dansyl-PE. The experimental setup in such experiments is as follows. Dansyl-labeled vesicles are first added to a peptide solution and, after an incubation time that is varied, unlabeled vesicles are added in excess. Peptide residing in the outer leaflet of the dansyl-labeled vesicles then rapidly equilibrates between the vesicle populations and relief from quenching is observed. Peptide that has translocated across the membrane, if any, is assumed to slowly revert to the exofacial monolayer, thus becoming free to diffuse to unlabeled vesicles, or even remains in the inner leaflet. However, the results from our experiments on GUVs suggest that peptide translocation across such membranes is a rapid process. If also translocation across LUV membranes was rapid, comparable in rate to the peptide redistribution between the vesicles, this method to assay peptide translocation would fail.

The results of the tryptophan quenching experiments with brominated lipids were very similar for all investigated peptides, indicating an average position of the Trp residues 10–11 Å from the lipid bilayer center corresponding to a penetration of approximately 5 Å into the hydrocarbon core region. As a control of the accuracy of our measurements, melittin was investigated. The tryptophan penetration depth of 10.2–10.9 Å is in excellent agreement with results from a study on vesicles very similar to ours containing 60% anionic DOPG [49] as well as with other results [30,50,51]. The Trp moiety in TOE is seemingly inserted somewhat deeper, residing 9.6 Å from the bilayer center according to DA and 10.2 Å according to PM. This is deeper than what has been previously reported by Ladokhin [30] for vesicles containing only brominated lipids (10.3–11 Å) and by Abrams and London [28] using spin-labeled phospholipids incorporated into DOPC vesicles (13.5 Å). At this point, we cannot explain this discrepancy, but it should be noted that the membranes used in this study contained 40% anionic lipid whereas those used in the other studies were neutral. Yau et al. [52] have shown that four Trp analogues, including the Trp chromophore indole as well as a Trp-containing tripeptide, exhibit a strong intrinsic preference for the membrane interfacial region, and thus

reside close to the glycerol groups. The authors hypothesize that there might exist a balance between the hydrophobic effect, pushing the residue towards the hydrocarbon region, and complex electrostatic interactions making the hydrated head-group region favorable. Furthermore, it has been established that aromatic residues, particularly tryptophan and tyrosine, in integral membrane proteins are often found at the membrane/water interface [53–55]. It has been suggested that these residues could serve to position the transmembrane helices within the bilayer [56]. Nevertheless, there are numerous reports on peptides that bind to lipid bilayers in predominantly α-helical conformations oriented parallel to the membrane surface where the insertion depths of the Trp residues are within the hydrocarbon core region [49,57–61].

Certainly, the amount of quencher present in the membrane affects the degree of quenching of tryptophan. Therefore, it is absolutely necessary to calibrate the concentration of brominated lipids in the different vesicles [27,28,62]. An easy way to circumvent the problem of controlling the exact concentration of quencher-carrying lipid is to investigate penetration depths in vesicles entirely composed of brominated lipids. However, this approach is not always applicable [25] or even desirable. Here we wish to relate the average insertion depths to the RET measurements in LUVs. Thus, vesicles that resemble those in the translocation studies as closely as possible were used. Additionally, the penetratin peptides used in this study have weak affinities for membranes containing only zwitterionic lipids. Consequently, vesicles with 30 mol% BrPC were used, and a careful assessment of BrPC concentrations in the stock solutions was necessary. The most common way to determine phospholipid content is the total phosphorous assay by Bartlett [63]. The method is time-consuming, can suffer from low reproducibility, and is extremely sensitive to trace amounts of inorganic phosphate [34,64]. The Stewart assay [34] is an alternative to Bartlett assay relying on the ability of phospholipids to form complexes with ammonium ferrothiocyanate in organic solution. The method is not sensitive to inorganic phosphate, but cannot be used if the sample contains mixtures of phospholipids. FTIR spectroscopy has previously been used to determine the phospholipid content in vegetable oils [64,65], and it was shown that reliable and reproducible results were obtained even though mixtures of phospholipids were present in the sample. Nzai et al. consider the 1200–970 cm^{-1} absorption band to be superior to the carbonyl stretch vibration at 1740 cm^{-1} since carbonyls in, for example, fatty acids can interfere in the analysis of vegetable oils. In our case, when determining phospholipid concentrations in pure samples, the carbonyl stretch vibration is the better choice since the 1200–970 cm^{-1} region has several overlapping vibrations that are complicated to resolve. Our findings indicate that FTIR measurements provide results similar to those obtained with Stewart assay, but with substantially lower spread.

We have previously observed by fluorescence microscopy that penetratin crosses the membranes of GUVs [18]. We here extended that work to include also PenArg, PenLys and Pen2W2F. Contrary to the situation in LUVs, all penetratin analogs rapidly crossed the barrier presented by GUV membranes and no differences in translocation properties between the peptides could be detected.

In a recent paper, we reported on large differences in the uptake in unfixed cells between the penetratin analogs studied here. Whereas penetratin and Pen2W2F upon association with the plasma membrane were apparently taken up via endocytosis, the internalization of PenArg via endocytosis was paralleled by another, energy-independent and non-endocytotic uptake mechanism. PenLys, on the other hand, was not at all taken up by cells. The arginines thus seem to play a key role in the interplay with the plasma membrane. In the present study, where we investigated the ability of the peptides to translocate across the membranes of large (100 nm) and giant (~tens of μm) unilamellar vesicles, no differences between the peptides could be detected as to explain the diverse behavior in cell internalization experiments. Instead, a large disparity was obtained between the model systems employed. While the peptides did not enter LUVs of any composition, including the soybean polar lipid extract used to prepare GUVs, the GUV membranes were more or less completely permeable to the peptides. Similar observations were made in a recent study by Fischer et al. [66], where a few low-molecular weight dyes and even proteins apparently traversed the membranes of GUVs prepared by electroformation, but did not penetrate through the bilayers of LUVs prepared by extrusion. Interestingly, the GUV membranes were less permeable to fluorescently labeled nucleotides and, as in our study, oligonucleotides. As reasoned in that report, the differences between the vesicle systems observed might originate from the more dynamic behavior of GUVs, manifested by their tendency to have undulated surfaces. However, little is currently known about the structural details of GUVs, rendering it difficult to answer the question whether the differences observed in terms of peptide permeability are actually due to the intrinsic properties of the two vesicle systems. In this context, although not likely to be of crucial importance, it is noteworthy that in the present study, the tools utilized to detect peptide translocation in the two vesicle systems set different limits as to which peptide to lipid ratios were applicable in the experiments.

In the light of the results presented here, it is likely that the very diverse uptake of the penetratin peptides in live cells originates from interactions with components other than the lipids in the plasma membrane. Nevertheless, it certainly could prove to be worthwhile trying to make the GUV membranes less permeable, e.g., by

including cholesterol in the GUV membranes [66], in search for correlations between the cellular uptake of CPPs and their interactions with lipid bilayers.

Acknowledgements

We thank Christina Brattwall, Petter Isakson and Åsa Nilsson for help with peptide synthesis and Prof. Kristina Luthman for putting a peptide synthesizer at our disposal. Karin Oscarsson and Åsa Nilsson are acknowledged for technical assistance and Michal Tokarz for help with preparation of GUVs. Dr. Bo Albinsson and Mattias Larsson are acknowledged for help with FTIR measurements. We thank Anders Karlsson, Roger Karlsson, Jon Sinclair and Max Davidsson for valuable discussions about GUVs. The confocal microscopy studies were conducted at the center for Biophysical Imaging at Chalmers, which is financed by SWEGENE.

References

[1] M. Lindgren, M. Hällbrink, A. Prochiantz, Ü. Langel, Cell-penetrating peptides, Trends Pharmacol. Sci. 21 (2000) 99–103.
[2] S.R. Schwarze, S.F. Dowdy, In vivo protein transduction: intracellular delivery of biologically active proteins, compounds and DNA, Trends Pharmacol. Sci. 21 (2000) 45–48.
[3] J.S. Wadia, S.F. Dowdy, Protein transduction technology, Curr. Opin. Biotechnol. 13 (2002) 52–56.
[4] P.M. Fischer, N.Z. Zhelev, S. Wang, J.E. Melville, R. Fåhraeus, D.P. Lane, Structure–activity relationship of truncated and substituted analogues of the intracellular delivery vector Penetratin, J. Pept. Res. 55 (2000) 163–172.
[5] E. Vivès, C. Granier, P. Prevot, B. Lebleu, Structure–activity relationship study of the plasma membrane translocating potential of a short peptide from HIV-1 Tat protein, Lett. Pept. Sci. 4 (1997) 429–436.
[6] E. Vivès, P. Brodin, B. Lebleu, A truncated HIV-1 Tat protein basic domain rapidly translocates through the plasma membrane and accumulates in the cell nucleus, J. Biol. Chem. 272 (1997) 16010–16017.
[7] M. Pooga, M. Hällbrink, M. Zorko, Ü. Langel, Cell penetration by transportan, FASEB J. 12 (1998) 67–77.
[8] S. Futaki, T. Suzuki, W. Ohashi, T. Yagami, S. Tanaka, K. Ueda, Y. Sugiura, Arginine-rich peptides. An abundant source of membrane-permeable peptides having potential as carriers for intracellular protein delivery, J. Biol. Chem. 276 (2001) 5836–5840.
[9] D. Derossi, A.H. Joliot, G. Chassaing, A. Prochiantz, The third helix of the Antennapedia homeodomain translocates through biological membranes, J. Biol. Chem. 269 (1994) 10444–10450.
[10] D. Derossi, S. Calvet, A. Trembleau, A. Brunissen, G. Chassaing, A. Prochiantz, Cell internalization of the third helix of the Antennapedia homeodomain is receptor-independent, J. Biol. Chem. 271 (1996) 18188–18193.
[11] P.A. Wender, D.J. Mitchell, K. Pattabiraman, E.T. Pelkey, L. Steinman, J.B. Rothbard, The design, synthesis, and evaluation of molecules that enable or enhance cellular uptake: peptoid molecular transporters, Proc. Natl. Acad. Sci. U. S. A. 97 (2000) 13003–13008.
[12] T. Suzuki, S. Futaki, M. Niwa, S. Tanaka, K. Ueda, Y. Sugiura, Possible existence of common internalization mechanisms among arginine-rich peptides, J. Biol. Chem. 277 (2002) 2437–2443.
[13] M. Lundberg, M. Johansson, Positively charged DNA-binding proteins cause apparent cell membrane translocation, Biochem. Biophys. Res. Commun. 291 (2002) 367–371.
[14] J.P. Richard, K. Melikov, E. Vives, C. Ramos, B. Verbeure, M.J. Gait, L.V. Chernomordik, B. Lebleu, Cell-penetrating peptides. A reevaluation of the mechanism of cellular uptake, J. Biol. Chem. 278 (2003) 585–590.
[15] P.E.G. Thorén, D. Persson, P. Isakson, M. Goksör, A. Önfelt, B. Nordén, Uptake of analogs of penetratin, Tat(48–60) and oligoarginine in live cells, Biochem. Biophys. Res. Commun. 307 (2003) 100–107.
[16] P.M. Fischer, E. Krausz, D.P. Lane, Cellular delivery of impermeable effector molecules in the form of conjugates with peptides capable of mediating membrane translocation, Bioconjug. Chem. 12 (2001) 825–841.
[17] M.A. Lindsay, Peptide-mediated cell delivery: application in protein target validation, Curr. Opin. Pharmacol. 2 (2002) 587–594.
[18] P.E.G. Thorén, D. Persson, M. Karlsson, B. Nordén, The Antennapedia peptide penetratin translocates across lipid bilayers—the first direct observation, FEBS Lett. 482 (2000) 265–268.
[19] S.C. Gill, P.H. Vonhippel, Calculation of protein extinction coefficients from amino-acid sequence data, Anal. Biochem. 182 (1989) 319–326.
[20] W.C. Wimley, S.H. White, Determining the membrane topology of peptides by fluorescence quenching, Biochemistry 39 (2000) 161–170.
[21] J.R. Lakowicz, Principles of Fluorescence Spectroscopy, 2nd ed., Kluwer Academic/Plenum Publishers, New York, 1999.
[22] D. Persson, P.E.G. Thorén, M. Herner, P. Lincoln, B. Nordén, Application of a novel analysis to measure the binding of the membrane-translocating Peptide penetratin to negatively charged liposomes, Biochemistry 42 (2003) 421–429.
[24] A.S. Ladokhin, P.W. Holloway, E.G. Kostrzhevska, Distribution analysis of membrane penetration of proteins by depth-dependent fluorescence quenching, J. Fluoresc. 3 (1993) 195–197.
[25] A.S. Ladokhin, Distribution analysis of depth-dependent fluorescence quenching in membranes: a practical guide, Methods Enzymol. 278 (1997) 462–473.
[26] A. Chattopadhyay, E. London, Parallax method for direct measurement of membrane penetration depth utilizing fluorescence quenching by spin-labeled phospholipids, Biochemistry 26 (1987) 39–45.
[27] F.S. Abrams, E. London, Calibration of the parallax fluorescence quenching method for determination of membrane penetration depth: refinement and comparison of quenching by spin-labeled and brominated lipids, Biochemistry 31 (1992) 5312–5322.
[28] F.S. Abrams, E. London, Extension of the parallax analysis of membrane penetration depth to the polar-region of model membranes—use of fluorescence quenching by a spin-label attached to the phospholipid polar headgroup, Biochemistry 32 (1993) 10826–10831.
[29] A.S. Ladokhin, Analysis of protein, peptide penetration into membranes by depth-dependent fluorescence quenching: theoretical considerations, Biophys. J. (1999) 946–955.
[30] A.S. Ladokhin, Evaluation of lipid exposure of tryptophan residues in membrane peptides and proteins, Anal. Biochem. 276 (1999) 65–71.
[31] T.J. McIntosh, P.W. Holloway, Determination of the depth of bromine atoms in bilayers formed from bromolipid probes, Biochemistry 26 (1987) 1783–1788.
[32] J.M. East, A.G. Lee, Lipid selectivity of the calcium and magnesium-ion dependent adenosine-triphosphatase, studied with fluorescence quenching by a brominated phospholipid, Biochemistry 21 (1982) 4144–4151.
[33] M.C. Wiener, S.H. White, Structure of a fluid dioleoylphosphatidylcholine bilayer determined by joint refinement of X-ray and neutron-diffraction data: 3. Complete structure, Biophys. J. 61 (1992) 434–447.

[34] R.R.C. New, in: R.R.C. New (Ed.), Liposomes—A Practical Approach, IRL Press/Oxford University Press, Oxford, 1990, pp. 108–109.
[35] M. Criado, B.U. Keller, A membrane-fusion strategy for single-channel recordings of membranes usually non-accessible to patch-clamp pipette electrodes, FEBS Lett. 224 (1987) 172–176.
[36] M. Karlsson, K. Nolkrantz, M.J. Davidson, A. Strömberg, F. Ryttsén, B. Åkerman, O. Orwar, Electroinjection of colloid particles and biopolymers into single unilamellar liposomes and cells for bioanalytical applications, Anal. Chem. 72 (2000) 5857–5862.
[37] M. Hoshiyama, K. Kubo, T. Igarashi, T. Sakurai, Complexation and proton dissociation behavior of 7-hydroxy-4-methylcoumarin and related compounds in the presence of beta-cyclodextrin, J. Photochem. Photobiol., A Chem. 138 (2001) 227–233.
[38] S.P. Bhamidipati, J.A. Hamilton, Interactions of lyso 1-palmitoylphosphatidylcholine with phospholipids—a C-13 and P-31 NMR-study, Biochemistry 34 (1995) 5666–5677.
[39] Y.V. Venkatachalapathi, M.C. Phillips, R.M. Epand, R.F. Epand, E.M. Tytler, J.P. Segrest, G.M. Anantharamaiah, Effect of end group blockage on the properties of a class-A amphipathic helical peptide, Proteins 15 (1993) 349–359.
[40] D. Persson, P.E.G. Thorén, P. Lincoln, B. Nordén, Vesicle membrane interactions of penetratin analogues, Biochemistry 43 (2004) 11045–11055.
[41] V.I. Razinkov, E.I. Hernandez-Jimenez, Mikhalyov II, F.S. Cohen, J.G. Molotkovsky, New fluorescent lysolipids: preparation and selective labeling of inner liposome leaflet, Biochim. Biophys. Acta 1329 (1997) 149–158.
[42] K. Matsuzaki, O. Murase, N. Fujii, K. Miyajima, Translocation of a channel-forming antimicrobial peptide, magainin 2, across lipid bilayers by forming a pore, Biochemistry 34 (1995) 6521–6526.
[43] J.D. Jones, T.E. Thompson, Spontaneous phosphatidylcholine transfer by collision between vesicles at high lipid-concentration, Biochemistry 28 (1989) 129–134.
[44] W.C. Wimley, T.E. Thompson, Transbilayer and interbilayer phospholipid exchange in dimyristoylphosphatidylcholine dimyristoylphosphatidylethanolamine large unilamellar vesicles, Biochemistry 30 (1991) 1702–1709.
[45] S. Kobayashi, K. Takeshima, C.B. Park, S.C. Kim, K. Matsuzaki, Interactions of the novel antimicrobial peptide buforin 2 with lipid bilayers: Proline as a translocation promoting factor, Biochemistry 39 (2000) 8648–8654.
[46] J. Everett, A. Zlotnick, J. Tennyson, P.W. Holloway, Fluorescence quenching of cytochrome-B5 in vesicles with an asymmetric transbilayer distribution of brominated phosphatidylcholine, J. Biol. Chem. 261 (1986) 6725–6729.
[47] C.E.B. Brattwall, P. Lincoln, B. Nordén, Orientation and conformation of cell-penetrating peptide penetratin in phospholipid vesicle membranes determined by polarized-light spectroscopy, J. Am. Chem. Soc. 125 (2003) 14214–14215.
[48] G. Drin, H. Demene, J. Temsamani, R. Brasseur, Translocation of the pAntp peptide and its amphipathic analogue AP-2AL, Biochemistry 40 (2001) 1824–1834.
[49] A.K. Ghosh, R. Rukmini, A. Chattopadhyay, Modulation of tryptophan environment in membrane-bound melittin by negatively charged phospholipids: implications in membrane organization and function, Biochemistry 36 (1997) 14291–14305.
[50] A.S. Ladokhin, P.W. Holloway, Fluorescence of membrane-bound tryptophan octyl ester: a model for studying intrinsic fluorescence of protein–membrane interactions, Biophys. J. 69 (1995) 506–517.
[51] Z. Oren, Y. Shai, Selective lysis of bacteria but not mammalian cells by diastereomers of melittin: structure–function study, Biochemistry 36 (1997) 1826–1835.
[52] W.M. Yau, W.C. Wimley, K. Gawrisch, S.H. White, The preference of tryptophan for membrane interfaces, Biochemistry 37 (1998) 14713–14718.
[53] M.B. Ulmschneider, M.S.P. Sansom, Amino acid distributions in integral membrane protein structures, Biochim. Biophys. Acta 1512 (2001) 1–14.
[54] C. Landolt-Marticorena, K.A. Williams, C.M. Deber, R.A.F. Reithmeier, Non-random distribution of amino acids in the transmembrane segments of human type I single span membrane proteins, J. Mol. Biol. 229 (1993) 602–608.
[55] G.V. Heijne, Membrane proteins: from sequence to structure, Annu. Rev. Biophys. Biomol. Struct. 23 (1994) 167–192.
[56] S. Mall, R.P. Sharma, J.M. East, A.G. Lee, Lipid–protein interactions in the membrane: studies with model peptides, Faraday Discuss. (1998) 127–136.
[57] J.E. Johnson, R.B. Cornell, Membrane-binding amphipathic alpha-helical peptide derived from CTP:phosphocholine cytidylyltransferase, Biochemistry 33 (1994) 4327–4335.
[58] C. Mangavel, R. Maget-Dana, P. Tauc, J.C. Brochon, D. Sy, J.A. Reynaud, Structural investigations of basic amphipathic model peptides in the presence of lipid vesicles studied by circular dichroism, fluorescence, monolayer and modeling, Biochim. Biophys. Acta 1371 (1998) 265–283.
[59] J. Hong, Z. Oren, Y. Shai, Structure and organization of hemolytic and nonhemolytic diastereomers of antimicrobial peptides in membranes, Biochemistry 38 (1999) 16963–16973.
[60] L. Voglino, S.A. Simon, T.J. McIntosh, Orientation of LamB signal peptides in bilayers: influence of lipid probes on peptide binding and interpretation of fluorescence quenching data, Biochemistry 38 (1999) 7509–7516.
[61] E. Breukink, C. van Kraaij, A. van Dalen, R.A. Demel, R.J. Siezen, B. de Kruijff, O.P. Kuipers, The orientation of nisin in membranes, Biochemistry 37 (1998) 8153–8162.
[62] E. London, A.S. Ladokhin, Measuring the depth of amino acid residues in membrane-inserted peptides by fluorescence quenching, Curr. Top. Membr. 52 (2002) 89–115.
[63] G.R. Bartlett, Phosphorus assay in column chromatography, J. Biol. Chem. 234 (1959) 466–468.
[64] J.M. Nzai, A. Proctor, Soy lecithin phospholipid determination by Fourier transform infrared spectroscopy and the acid digest arsenomolybdate method: a comparative study, J. Am. Oil Chem. Soc. 76 (1999) 61–66.
[65] J.M. Nzai, A. Proctor, Determination of phospholipids in vegetable oil by Fourier transform infrared spectroscopy, J. Am. Oil Chem. Soc. 75 (1998) 1281–1289.
[66] A. Fischer, T. Oberholzer, P.L. Luisi, Giant vesicles as models to study the interactions between membranes and proteins, Biochim. Biophys. Acta, Biomembr. 1467 (2000) 177–188.